Luminescence Properties of Rhodamine 6G Intercalated in Surfactant/Clay Hybrid Thin Solid Films

7 AUTHORS, INCLUDING:

Ryo Sasai
Shimane University
119 PUBLICATIONS   **1,315** CITATIONS

SEE PROFILE

Fernando López Arbeloa
Universidad del País Vasco / Euskal Herriko U…
110 PUBLICATIONS   **2,928** CITATIONS

SEE PROFILE

Virginia Martínez Martínez
Universidad del País Vasco / Euskal Herriko U…
45 PUBLICATIONS   **1,176** CITATIONS

SEE PROFILE

Katsuhiko Takagi
Nagoya University
113 PUBLICATIONS   **2,250** CITATIONS

SEE PROFILE

Luminescence Properties of Rhodamine 6G Intercalated in Surfactant/Clay Hybrid Thin Solid Films

Ryo Sasai,*,† Nobuo Iyi,‡ Taketoshi Fujita,‡ Fernando López Arbeloa,§
Virginia Martínez Martínez,§ Katsuhiko Takagi,‖ and Hideaki Itoh†

*Research Center for Advanced Waste and Emission Management (ResCWE),
Nagoya University, Furo-cho, Chikusa-ku, Nagoya 464-8603, Japan, Advanced Materials
Laboratory (AML), National Institute for Materials Science (NIMS), Namiki 1-1, Tsukuba,
Ibaraki 305-0044, Japan, Departamento de Química Física, Universidad del País Vasco-EHU,
Apartado de Correos 644, Bilbao 48080, Spain, and Department of Crystalline Materials
Science, Graduate School of Engineering, Nagoya University,
Furo-cho, Chikusa-ku, 464-8603, Japan*

To develop the solid-state laser oscillator based on laser dye compounds, the incorporation of rhodamine 6G (R6G, a laser dye) in cetyltrimethylammonium (CTA$^+$) cationic surfactant/montmorillonite clay hybrid (HpC) thin solid films was investigated. The R6G/HpC samples were prepared by immersing the HpC films into a R6G aqueous solution with various concentration. X-ray diffraction patterns of the films of HpC, measured before and after the intercalation of R6G, proved the coexistence of both the dye and surfactant in clay interlayer spaces. All prepared thin films exhibited luminescence. It indicates that CTA$^+$ molecules play a role as a partial suppressor of the aggregation of R6G molecules which prevents fluorescence. Moreover, the luminescence property of the present thin films was observed to be dependent on the co-intercalated degree of R6G molecules, indicating that the R6G intercalating in HpC interlayer space molecules exist as two or more luminescence species in the clay interlayer space.

Introduction

Commercially available tunable lasers generally use liquid-state active media, which require circulating laser dye solutions. However, these types of laser oscillators have serious drawbacks because they involve a large circulator with toxic solvents in most case and careful maintenances. The development of solid-state tunable lasers, with interesting technological innovations such as compactness or miniaturization, could solve these problems. Tunable solid-state lasers can be obtained by the incorporation of laser dyes as guest compounds in host solid materials. So far, several light-emitting solid systems based on the inclusion of laser dyes in organic and in inorganic solid matrixes have been described in the literature.[1−19]

Rhodamine 6G (R6G) dye, a typical laser dye, exhibits a high fluorescence band with a fluorescence quantum yield around 0.7 in dilute solution.[20] However, this emission efficiency is drastically reduced in concentrated solutions, in the solid state (both crystalline and powdered forms), or in solid host materials, as a consequence of the high tendency of R6G dye easily to form H-type sandwich aggregates (H-aggregates) without luminescence ability and with activity as an efficient quenchers for the monomer fluorescence.[13−17] Therefore, to prevent dye aggregation and to get luminescence ability from laser dyes in solid state, it is necessary to isolate the individual R6G molecules adsorbed in the solid materials. In this sense, R6G molecules have been incorporated in hybrid organic/inorganic systems, such as organophilic clay systems (so-called hydrophobic clays, HpC) obtained by the substitution of the inorganic exchangeable cations of clays by organic surfactants cations.[21−23]

Cation-exchangeable clay minerals such as montmorillonite, saponite, hectorite, and taeniolite, which are

* To whom correspondence should be addressed. Tel: +81-52-789-5851. Fax: +81-52-789-5849. E-mail: rsasai@rescwe.nagoya-u.ac.jp.
† ResCWE, Nagoya University.
‡ National Institute for Materials Science.
§ Universidad del País Vasco-EHU.
‖ Graduate School of Engineering, Nagoya University.

(1) Yang, Y.; Wang, G. D.; Qian, Z. Y.; Wang, Y.; Hong, Z.; Fan, X. P.; Chen, J. *Mater. Lett.* **2002**, *57*, 660.
(2) Zhu, X. L.; Lo, D. *Appl. Phys. Lett.* **2002**, *80*, 917.
(3) Nonell, S.; Marti, C.; Garcia-Moreno, I.; Costela, A.; Satre, R. *Appl. Phys. B* **2001**, *72*, 355.
(4) Yap, S. S.; Tou, T. Y.; Ng, S. W. *Jpn. J. Appl. Phys., Part 1* **2000**, *39*, 5855.
(5) Holzer, W.; Gratz, H.; Schmitt, T.; Penzkofer, A.; Costela, A.; Garcia-Moreno, I.; Sastre, R.; Duarte, F. J. *Chem. Phys.* **2000**, *256*, 125.
(6) Costela, A.; Garcia-Moreno, I.; Figuera, J. M.; Amat-Guerri, F.; Sastre, R. *Laser Chem.* **1998**, *18*, 63.
(7) Lo, D.; Lam, K.; Ye, C.; Lam, K. S. *Opt. Commun.* **1998**, *156*, 316.
(8) Ramalingam, A.; Somasundaram, S.; Sathyabhma, S.; Palanisamy, P. K.; Masilamini, V. *Indian J. Pure Appl. Phys.* **1998**, *36*, 310.
(9) Hu, L. L.; Jiang, Z. H. *Opt. Commun.* **1998**, *148*, 275.
(10) Yamamoto, T.; Fujii, A.; Tagaya, Teramoto, S.; Nihei, E.; Koike, Y.; Sasaki, K. *Electron. Commun. Jpn. 2* **1995**, *78*, 36.
(11) Ammer, F.; Penzkofer, A.; Weidner, P. *Chem. Phys.* **1994**, *192*, 325.
(12) Enmanji, K. *Nippon Kagaku Kaishi* **1994**, 1046.
(13) Iyi, N.; Sasai, R.; Fujita, T.; Deguchi, T.; Sota, T.; López Arbeloa, F.; Kitamura, K. *Appl. Clay Sci.* **2002**, *22*, 125.
(14) Sasai, R.; Fujita, T.; Iyi, N.; Itoh, H.; Takagi, K. *Langmuir* **2002**, *18*, 6578.
(15) Chen, G. M.; Iyi, N.; Sasai, R.; Fujita, T.; Kitamura, K. *J. Mater. Res.* **2002**, *17*, 1035.
(16) Fujita, T.; Iyi, N.; Kosugi, T.; Ando, A.; Deguchi, T.; Sota, T. *Clays Clay Miner.* **1997**, *45*, 77.
(17) Ogawa, M.; Kawai, R.; Kuroda, K. *J. Phys. Chem.* **1996**, *100*, 16218.
(18) Ito, K.; Zhou, N.; Fukunishi, K.; Fujiwara, Y. *J. Imaging Sci. Technol.* **1994**, *38*, 575.
(19) Schulz-Ekloff, G.; Wohrle, D.; van Duffel, B.; Schoonheydt, R. A. *Microporous Mesoporous Mater.* **2002**, *51*, 91.
(20) Santhi, A.; Umadevi, M.; Ramakrishnan, V.; Radhakrishnan, P.; Nampoori, P. V. *Spectrochim. Acta, Part A* **2003**, in press.
(21) Usami, H.; Takagi, K.; Sawaki, Y. *Bull. Chem. Soc. Jpn.* **1991**, *47*, 799.
(22) Ghosh, P. K.; Bard, A. J. *J. Phys. Chem.* **1984**, *88*, 5519.
(23) Endo, T.; Sato, T.; Shimada, M. *J. Phys. Chem. Solid* **1986**, *47*, 799.

negatively charged layered materials, possess two-dimensional spaces in which ionic or polar organic molecules can be accommodated by the ion-exchange reaction.[24-31] It is well-known that the intercalation of guest organic dyes forms various types of self-assembled structure or aggregates such as lamella, interdigitated monolayers, and H-type or J-type head-to-tail aggregates (J-aggregates) as a consequence of their interaction with the highly negatively charge densities on the clay layer surface.[24-31] Many researchers have investigated the synthesis and characterization of these functional dye/clay hybrid materials.[30-46] Thus, López Arbeloa et al.[47-54] have studied the aggregation of several rhodamines adsorbed into different smectite-type clays in diluted aqueous suspensions by spectroscopic analysis. From these works, the dimers, trimers, and/or higher-order sandwich and/or head-to-tail aggregates adsorbed in the external surface and/or interlayer space were characterized depending on the nature of the clay and the hydrophobic character of the dye. In previous papers, we reported by polarization absorption spectroscopy the details of self-assembled structure of R6G and related compounds intercalated into the interlayer space of thin films of various clay minerals.[13-15] Nonsignificant fluorescence was observed from these thin films, since rhodamine dyes were present as higher-order H-aggregates. Endo et al.[23] have also reported that the presence of ethanol molecules in rhodamine-dye/smectite-clay systems provides solid-state materials with emitting ability. However, these systems do not have adequate performance as practical materials, because it is difficult to control the amount of the co-intercalated ethanol molecules.

In a previous study,[46] we successfully co-intercalated R6G dye in a hybrid cetyltrimethylammonium montmorillonite HpC solid material with light-emitting ability. However, this hybrid material was prepared only as powder. Therefore, it should be necessary to establish the technique for preparing thin solid films or bulk modules for using as practical fluorescent materials. In this study, we attempted to prepare the R6G/cationic surfactant/clay hybrid thin solid film with light-emitting ability. Furthermore, the light-emitting ability and the details of self-assembled structure of the prepared hybrid thin solid films were investigated.

Experimental Section

Materials. Purified standard sodium montmorillonite (Mont: Tsukinuno, $Na^{0.33+}[(Al_{1.67}Mg_{0.33})Si_4O_{10}(OH)_2 \cdot nH_2O]^{0.33-}$; ca. 2 wt % Fe was included) with a cationic-exchange capacity (CEC) of 1.19 mequiv/g obtained from the Clay Science Society of Japan was used without further purification. Cetyltrimethylammonium bromide (CTA^+Br^-) and laser grade R6G were purchased from Tokyo Kasei Chemical Industry Co., Ltd., and Lambda Physick, respectively, and they were used without further purification.

Preparation of Hybrid Thin Solid Films. CTA^+/Mont hybrid powder, so-called hydrophobic clay (HpC), was prepared by filtration, rinsing, and drying of the white precipitate obtained by adding CTA^+Br^- molecules (1.19 mmol) to 50 g/L of Mont aqueous suspension. The amount of the incorporated CTA^+ molecules/CEC was about unity. The HpC thin solid films were prepared by casting 0.5 mL of a clear HpC toluene suspension (10 g/L) on the glass plate and dried in vacuo at room temperature. R6G was incorporated by immersing overnight the HpC thin solid film into 20 mL of a R6G aqueous solution with an appropriate dye concentration at 60 °C. The elaborated R6G/HpC thin film was rinsed in distilled and deionized water and in ethanol and then dried at 60 °C in vacuo. The amount of the incorporated R6G molecules was estimated from absorbance at 526 nm of R6G remaining in the aqueous solution obtained after the immersing process.

Characterization. Powder X-ray diffraction (XRD) analysis of the R6G/HpC hybrid thin solid films was carried out with a RINT-2000 diffractometer (RIGAKU) using a Cu Kα radiation source. The UV/vis isotropic and polarized absorption spectra of R6G/HpC films were recorded on a JASCO V-550 spectrophotometer with a JASCO polarizer unit attachment (model RSH-452). The fluorescence spectra of the R6G/HpC thin films were registered on a Shimadzu RF-5000 in the front-face configutarion, orientating the normal to the supported glass plate by 40 and 50° with respect to the excitation beam and the detecting arm, respectively. The excitation was performed at 495 nm, and the Rayleigh light-scattering was compensated by subtracting the detected signal of a pure HpC films (without dye) from the experimental fluorescence spectra.

Results and Discussion

Incorporation of R6G Molecules into HpC Thin Solid Films. Figure 1 shows the relationship between the R6G concentration of immersing solution and amount of incorporated R6G molecules/CEC, [R6G]/[CEC]. For diluted immersion solutions in the $<10^{-5}$ mol/L range, the amount of adsorbed R6G molecules linearly increased with the concentration of the dye solution. This result indicates that the amount of incorporated R6G molecules could be controlled freely by changing the concentration

(24) Grim, R. E. *Clay Mineralogy*; McGraw-Hill: New York, 1953.
(25) Whitingham, M. S.; Jacobson, A. J. *Intercalation Chemistry*; Academic Press: New York, 1982.
(26) Alberti, G.; Bein, T. *Comprehensive Supramolecular Chemistry*; Pergamon: Oxford, U.K., 1996; Vol.7.
(27) Mortland, M. M.; Fripiat, J. J.; Chaussidon, J.; Oytterhoeven, J. *J. Phys. Chem.* **1963**, *67*, 248.
(28) Farmer, V. C.; Mortaland, M. M. *J. Chem. Soc. A* **1966**, 344.
(29) Weiss, A. *Clays Clay Miner.* **1963**, *10*, 191.
(30) *Kikan Kagaku Sosetu No. 21, Microporous Crystals*; edited by the Chemical Society of Japan; Japan Scientific Societies Press: Tokyo, 1994.
(31) *Kikan Kagaku Sosetsu No. 42, Muki-yuuki Nano Fukugoutai Busshitsu*; edited by the Chemical Society of Japan; Japan Scientific Societies Press: Tokyo, 1999.
(32) Takagi, K.; Kurematsu, T.; Sawaki, Y. *J. Chem. Soc., Perkin Trans. 2* **1991**, 1517.
(33) Ogawa, M.; Fujii, K.; Kuroda, K.; Kato, C. *Mater. Res. Soc. Symp. Proc.* **1991**, *233*, 89.
(34) Ogawa, M.; Ishikawa, A. *J. Mater. Chem.* **1998**, *8*, 463.
(35) Seki, T.; Ichimura, K. *Macromolecules* **1990**, *23*, 31.
(36) Sasai, R.; Ogiso, H.; Shindachi, I.; Shichi, T.; Takagi, K. *Mol. Cryst. Liq. Cryst.* **2000**, *56*, 6979.
(37) Sasai, R.; Ogiso, H.; Shindachi, I.; Shichi, T.; Takagi, K. *Tetrahedron* **2000**, *645*, 39.
(38) Sasai, R.; Itoh, H.; Shindachi, I.; Shichi, T.; Takagi, K. *Chem. Mater.* **2001**, *13*, 2012.
(39) Cooper, S.; Dutta, P. K. *J. Phys. Chem.* **1990**, *94*, 114.
(40) Ogawa, M.; Takahashi, M.; Kuroda, K. *Chem. Mater.* **1994**, *6*, 715.
(41) Sasai, R.; Shichi, T.; Gekko, K.; Takagi, K. *Bull. Chem. Soc. Jpn.* **2000**, *73*, 1925.
(42) Ogawa, M.; Takahashi, M.; Kato, C.; Kuroda, K. *J. Mater. Chem.* **1994**, *4*, 519.
(43) Ogawa, M.; Handa, T.; Kuroda, K. Kato, C.; Tani, T. *J. Phys. Chem.* **1992**, *96*, 8116.
(44) Sakoda, K.; Kominami, T. *Chem. Phys. Lett.* **1993**, *216*, 270.
(45) Fujita, T.; Iyi, N.; Klapyta, Z. *Mater. Res. Bull.* **1998**, *33*, 1693.
(46) Sasai, R.; Iyi, N.; Fujita, T.; Takagi, K.; Itoh, H. *Chem. Lett.* **2003**, *32*, 550.
(47) Tapia Estévez, M. J.; López Arbeloa, F.; López Arbeloa, T.; López Arbeloa, I.; Schoonheydt, R. A. *Clay Miner.* **1994**, *29*, 105.
(48) Tapia Estévez, M. J.; López Arbeloa, F.; López Arbeloa, T.; López Arbeloa, I. *J. Colloid Interface Sci.* **1994**, *162*, 412.
(49) López Arbeloa, F.; López Arbeloa, T.; López Arbeloa, I. *Trends Chem. Phys.* **1996**, *4*, 191.
(50) López Arbeloa, F.; Tapia Estévez, M. J.; López Arbeloa, T.; López Arbeloa, I. *Clay Miner.* **1997**, *32*, 97.
(51) López Arbeloa, F.; López Arbeloa, T.; López Arbeloa, I.; Costela, A.; Garcia-Moreno, I.; Figuera, J. M.; Amat-Guerri, F.; Sastre, R. *J. Lumin.* **1997**, *75*, 309.
(52) López Arbeloa, F.; Herrán Martínez, J. M.; López Arbeloa, T.; López Arbeloa, I. *Langmuir* **1998**, *14*, 4566.
(53) Chaudhuri, R.; López Arbeloa, F.; López Arbeloa, I. *Langmuir* **2000**, *16*, 1285.
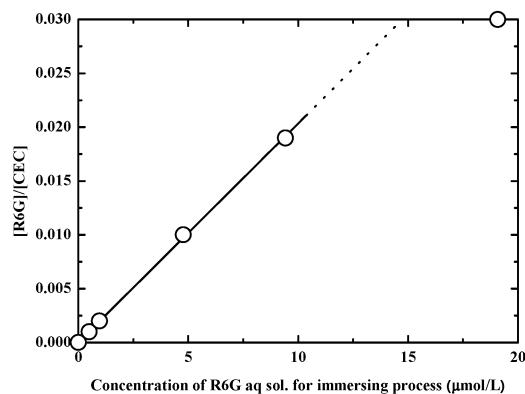(54) López Arbeloa, F.; Martínez Martínez, V.; Bañuelos Prieto, J.; López Arbeloa, I. *Langmuir* **2002**, *18*, 2658.

Figure 1. Dependence of the molar ratio of the intercalated R6G cation over the total CEC of HpC films, [R6G]/[CEC], with the dye concentration of the immersion solution.
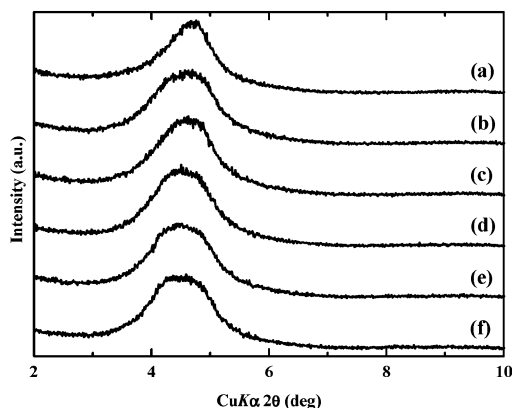
Figure 2. X-ray diffraction profiles of the R6G/HpC hybrid thin solid films. [R6G]/[CEC] = 0 (a), 0.001 (b), 0.002 (c), 0.010 (d), 0.019 (e), and 0.030 (f).

of the immersing solution. Therefore, it will be possible to prepare R6G/HpC hybrid thin solid film with the desired amount by using the present preparation procedure.

XRD Profiles of R6G/HpC Hybrid Thin Solid Films. The XRD profiles of the R6G/HpC hybrid thin films are shown in Figure 2. The basal diffraction peak of hybrid thin films shifts to lower diffraction angles and its half-bandwidth becomes wider by increasing the content of R6G molecules in the film, but its intensity does not depend on the amount of incorporated R6G molecules. These results indicate that the incorporated R6G molecules increase of an average value of interlayer space of HpC film. Therefore, it can be considered that most of incorporated R6G molecules exist in the HpC interlayer space together with CTA$^+$ molecules. Indeed, the R6G molecules adsorbed on the surface of HpC films are thought to be eliminated by the washing procedure of the sample preparation.

Only the basal d_{001} diffraction peak was observed for all of XRD profiles of R6G/HpC films (Figure 2), indicating that the clay layers could be aligned on a parallel with a the glass plate surface in all of the hybrid thin solid films prepared by the present procedure. Thus, the R6G molecules intercalated into HpC interlayer space could be also aligned on a certain angle with the glass plate because the intercalated guest molecules were oriented in clay interlayer space almost as in the case of the guest/clay hybrid materials. In this case, the R6G/HpC films have to be considered as an anisotropic system and would give a different response with respect to the plane of the polarization for linearly polarized incident light.
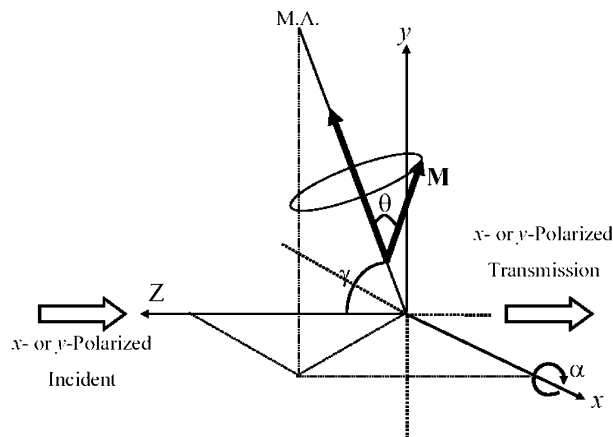
Figure 3. Schematic illustration for the polarized absorption measurements. The sample film was set parallel to the *xy*-plane and rotates an α-angle around the *x*-axis. The molecular axis (MA) of the oriented dye molecules forms a *γ*-angle with respect to the normal to the films and a *θ*-angle with respect to the dipole transition moment (**M**) of the dye.
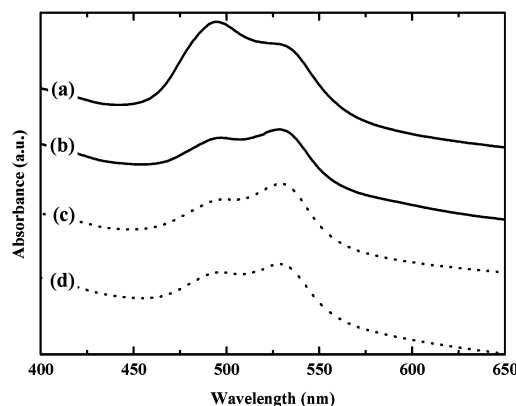
Figure 4. Visible polarized absorption spectra of the R6G/HpC hybrid thin solid film with [R6G]/[CEC] = 0.019: absorption spectra for *y*-polarized light (a, b); absorption spectra for *x*-polarized light (c, d). Incident α-angle was 0 (b, d) and 40° (a, c).

UV/Vis Polarized Absorption Spectra of the R6G/HpC Hybrid Thin Solid Films. Figure 3 shows a schematic illustration of the measurement of UV/vis absorption spectra with *x*- and *y*-polarized incident light through the *z*-axis. If the molecular axis (MA) of the dye has a preferential orientation with respect to the normal to the films (the *γ* angle in Figure 3), then the absorbance of the sample with respect to the *x*- and *y*-polarized light would be different depending on the twisted angle of the film with respect to the *x*- (or *y*-) axis.

Figure 4 shows an illustrative change in the absorption spectrum of a R6G/HpC thin film with [R6G]/[CEC] = 0.019 for *x*- and *y*-polarized incident light and films oriented perpendicular and twisted by 40° through the *x*-axis (α value in Figure 3 equal to 0 and 40°). In fact, the absorption spectrum of R6G could be barely changed by twisting the α angle in the case of the *x*-polarized incident light, while the absorbance at 490 nm, observed as a shoulder in the absorption spectrum at α = 0°, increases by increasing the α value with *y*-polarized light as an incident light. This behavior became marked with an increase in the [R6G]/[CEC] value, but it was almost not observed for samples with a low content in R6G, [R6G]/[CEC] ≤ 0.002.

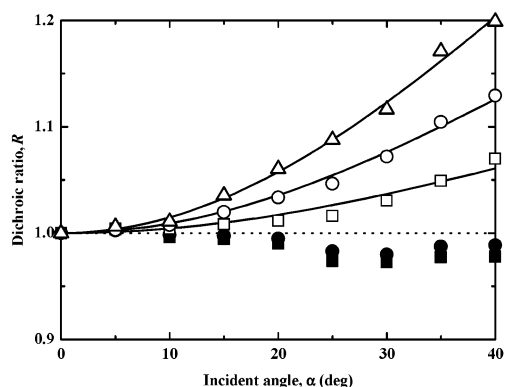The 490 nm absorption band, showing this interesting behavior with respect to the linearly polarized light, can

Figure 5. Dependence of the dichroic ratio, R, at 490 nm (---) with the incident α-angle for [R6G]/[CEC] = 0.001 (■), 0.002 (●), 0.010 (□), 0.019 (○), and 0.030 (△) samples.

be identified with the absorption peak of an H-type dimer of R6G with sandwich structure reported by López et al.[47−52] and our previous paper.[14] Therefore, it can be concluded that, for high enough content of dye molecules [R6G]/[CEC] ≥ 0.010, the adsorption of R6G molecules in HpC films leads to H-type R6G dimers with a sandwich structure, which are regularly aligned in the clay interlayer space.

This aligned γ angle can be estimated from the evolution of the dichroic ratio (R), defined as the ratio between the absorbance of the sample for y-polarized (A_y) with respect to x-polarized light (A_x), with the twisted α angles through the x-axis. If γ is the angle between the normal to the film plane and the molecular axis of the dye (the tilt angle of the long axis of the xanthene ring with respect to the plane of the HpC film) and θ is the angle between the molecular axis and the dipole moment transition of the dye, then the dichroic ratio $R = A_y/A_x$ for any twisted α-angle is given by

$$R = A_y/A_x = \{2[\sin^2\theta + \sin^2\alpha(3\cos^2\theta - 1)] - (3\sin^2\alpha - 1)(3\cos^2\theta - 1)\sin^2\gamma\}/ \{2\sin^2\theta + (2 - 3\sin^2\theta)\sin^2\gamma\} \quad (1)$$

In the case of the R6G molecule, the optical transition moment of the absorption in the visible range is along the long molecular axis; i.e., $\theta = 0°$. Therefore, eq 1 can be written as follows:

$$R = [2\sin^2\alpha - (3\sin^2\alpha - 1)\sin^2\gamma]/\sin^2\gamma \quad (2)$$

Figure 5 shows the dependence of the dichroic ratios R at 490 nm with the twisted α angle for R6G/HpC hybrid thin films in various [R6G]/[CEC] values. In the case of extremely low [R6G]/[CEC] values ([R6G]/[CEC] ≤ 0.002), the R value is slightly lower than the unity, suggesting a random distribution of the adsorbed R6G molecules in the HpC films or an alignment of R6G molecules slightly lower than the magic angle ($\gamma = 35.3°$: this value is at R =1). For more concentrated films [R6G]/[CEC] > 0.01, the R value is higher than the unity and increases with the α-angle, indicating a higher aligned γ-angle with respect to the normal to the film. The tilt angles of the molecular axis with respect to the film plane ($\Theta_T = 90 - \gamma$) can be estimated from the γ-angles obtained by fitting the dependence of R value with the α-angle (eq 2) and are shown in Table 1.

From experimental results shown in Table 1, it can be concluded that the γ (or the $\Theta_T = 90 - \gamma$) value decreases (increases) as increasing the R6G content in HpC films,

Table 1. Orientation Angle, Θ_T, of the Incorporated R6G Molecules with Respect to the HpC Film Plane for Different R6G/HpC Concentrations[a]

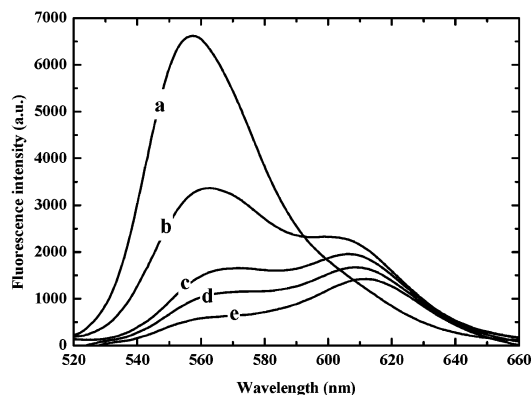|	[R6G]/[CEC]				
	0.001	0.002	0.010	0.019	0.030
Θ_T (deg)	(34.2)	(34.6)	37.1	38.9	40.8

[a] Parenthetic values are provisional data.

Figure 6. Fluorescence spectra of R6G/HpC hybrid thin solid films. [R6G]/[CEC] = 0.001 (a), 0.002 (b), 0.010 (c), 0.019 (d), and 0.030 (e).

i.e., the [R6G]/[CEC] value. These results suggest that the R6G molecule gradually raises itself up with increasing the amount of adsorbed R6G molecules. The occupied volume/R6G molecule is larger than that of CTAB molecule from the theoretical calculation. Therefore, the vacant space within HpC interlayer space decreases with an increase in the amount of the intercalated R6G cations when the R6G molecules are intercalated in the HpC interlayer space. For cancellation of steric hindrance between R6G and CTA$^+$ molecules and/or R6G molecules arisen by the intercalation of R6G molecules, the Θ_T values will increase, and then the partial enlargement of the interlayer distance could be observed. This conclusion is supported by X-ray diffraction data (Figure 2), in which an augmentation of the interlayer space by increasing the [R6G]/[CEC] ratio can be drawn out.

Fluorescence Spectra of R6G/HpC Hybrid Thin Solid Films. Each R6G/HpC thin films exhibited a fluorescence spectrum shown in Figure 6. These results indicate that it is possible to prepare thin solid films with luminescence ability by the incorporation of small amount of R6G molecules with the HpC hybrid by the present procedure. However, the luminescence characteristics (wavelength and efficiency) of each film depend on the amount of adsorbed R6G molecules.

In the extremely low concentrations ([R6G]/[CEC] ≤ 0.001), only the fluorescence peak of R6G monomer was predominantly observed around 555 nm.[14] Therefore, most of the incorporated R6G molecules exist as monomer species in the HpC interlayer space. Considering the above results of UV/vis polarized absorption measurements, the adsorption of R6G molecules as isolated monomers in the HpC interlayer space could have a random distribution or an orientation angle slightly lower than the magic angle $\gamma = 35.3°$ (Table 1).

However, this fluorescence peak originated from the isolated R6G molecules gradually disappeared and a new fluorescence band appears at higher wavelength (around 610 nm) by increasing the R6G content in the HpC films, Figure 6. The intensity of this new fluorescence peak gradually decreases by increasing the [R6G]/[CEC] value. The dependence of the fluorescence intensity ratio at 550
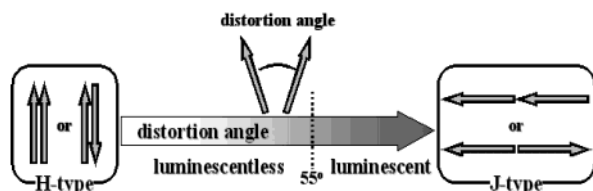
Figure 7. Schematic models of perfect H-type sandwich and J-type aligned head-to-tail dimers.

over that at 610, $I_{fl}(555)/I_{fl}(610)$, with the amount of adsorbed R6G indicated that the new luminescence species should be produced to the detriment of the R6G monomers and could be attributed to a R6G aggregate as a consequence of the intermolecular interaction between the R6G molecules intercalated in the HpC interlayer space, favored in high dye concentration films. Considering the above results obtained from polarized absorption light, this fluorescence should be ascribed to the emission of the R6G dimer. Taking into account the exciton theory,[55] a perfect sandwich dimer does not emit. It is well-known that there are two extreme kinds of molecular dimers (Figure 7): that with a perfect sandwich structure (H-type) and that with a perfect aligned dipole moments (J-type structure). The former is characterized by an intense absorption band placed at higher energies than the monomer band (the H-band), whereas the later is fluorescent with absorption and fluorescence bands at lower energies (the J-band) with respect to the corresponding monomeric band. If the configuration of two R6G molecules was distorted and a nonperfect sandwich (twisted) H-type dimer was produced, this species could possess both H- and J-bands and could exhibit the fluorescence peak at longer wavelength than the monomeric band. Such species are well-known to possess fluorescence ability, when the distortion angle between the dipole moments of the two

monomeric units is higher than 55°.[56] These kinds of aggregates are common in isocyanine and thiacarbocyanine derivatives.[57,58] Consequently, it can be concluded that the fluorescence observed around 600 nm for the R6G/HpC films with [R6G]/[CEC] > 0.002 could be caused by the twisted H-type dimer with the distortion angle more than 55°. This distortion of R6G dimer in the HpC interlayer space may be related the irregularity of tilt angle against clay surface of R6G molecule incorporated as monomer, but further detailed analysis will be necessary for clarify the reason of this distortion.

Conclusions

We successfully prepared fluorescent R6G/HpC hybrid thin solid films by immersing the supported HpC films into R6G aqueous solutions. The amount of the adsorbed R6G in the HpC film is easily controlled by changing the concentration of the dye in the immersion solution. Absorption spectra suggest the presence of a monomer and H-type dimer of R6G in the interlayer space of HpC films. The adsorbed R6G dimers have a preferential orientation in the films with a tilt angle with respect to the film plane around 40°, which increases with the dye content. Monomers are randomly distributed or with a tilt angle close to the magic one 35.3°. All prepared films present fluorescent ability. For diluted R6G films ([R6G]/[CEC] < 0.001), the emission at around 555 nm is from R6G momomers, whereas a fluorescence band of R6G aggregates is observed at around 610 nm for films with more concentrated R6G molecules. This emission could be caused by the J-band of a distorted sandwich R6G dimer species adsorbed in HpC interlayer space.

(55) Kasha, M. *Radiat. Res.* **1963**, *20*, 55.

(56) del Monte, F.; Levy, D. *J. Phys. Chem. B* **1998**, *102*, 8036.
(57) Misawa, K.; Ono, H.; Minoshima, K.; Kobayashi, T. *Appl. Phys. Lett.* **1993**, *63*, 577.
(58) Scheblykin, I. G.; Drobizhev, M. A.; Varnavsky, O. P.; Van der Auweraer, M.; Vitukhnovsky, A. G.; *Chem. Phys. Lett.* **1996**, *261*, 181.